R-ProjNet: an optimal rotated-projection neural network for wood segmentation from point clouds

Sheng Xu, Xin Li, Hongxin Yang & Shanshan Xu

Published online: 28 Dec 2022.

Submit your article to this journal

Article views: 81

View related articles

View Crossmark data

Taylor & Francis
Taylor & Francis Group

Check for updates

R-ProjNet: an optimal rotated-projection neural network for wood segmentation from point clouds

Sheng Xu [ID][a], Xin Li[a], Hongxin Yang[b] and Shanshan Xu[a]

[a]College of Information Science and Technology, Nanjing Forestry University, Nanjing, China; [b]Department of Geomatics Engineering, University of Calgary, Calgary, Canada

ABSTRACT

This work aims to provide a deep learning framework to segment woods from tree point clouds. We develop a novel preprocessing layer before the classical sampling and convolution structure called the projection layer to organize 3D point clouds into 2D points. Input data are transformed into projection data along axis and planes for the subsequent convolution process, which helps decrease the complexity of networks. In order to obtain optimal and effective projection data for capturing local features, we formulate the 2D transformation in the learning process using two learnable angle parameters. The projection map is updated in the learning process for capturing geometric structure information, which plays an important role in wood point segmentation. Experiments show that we have achieved the loss and misclassification error of 0.41% and 8%, respectively, on wood points extraction from handheld laser scanning data. Besides, we also achieve the correctness, completeness and *F*-score of 90.4%, 91.5% and 0.91, respectively, in a public vehicle laser scanning dataset.

1. Introduction

Nowadays, laser scanning technology has played a significant role in mapping 3D space information of vegetation, such as the crown delineation (Sun et al. 2022), instance segmentation (Wang 2020) and wood-leaf separation (Hu, Pan, and Zhong 2020). As one of the key steps in vegetation mapping, the wood point extraction is the foundation of tree structure analysis. Commonly used LiDAR (Light Detection and Ranging) devices are mounted on airborne systems (Yun et al. 2021), terrestrial systems (Hui et al. 2021), vehicle systems (Chen et al. 2019) and handheld systems (Vatandaşlar and Zeybek 2021; Balenović et al. 2021). There are lots of machine learning methods for the task of classifying wood points to study tree structures.

In terms of the classical methods, the existing algorithms are often in two steps, i.e., feature extraction and classifier training. In the method of Li et al. (2020), they present 16 local statistical geometrical features from the sphere domain of each point to represent the input data and use classical machine learning methods to separate point clouds directly. Hu, Pan, and Zhong (2020) develop a framework for the wood separation by

---

formulating locally convex connected patches to segment branch points from the organized supervoxels, and then they use the *k*-means++ clustering algorithm to further segment connected leaves and branches. Moorthy et al. (2020) combine geometrical features defined by radially bounded nearest neighbours at multiple spatial scales and then choose traditional machine learning methods, e.g., random forest, to split wood points.

In terms of the deep learning approaches, the commonly used structure is the convolutional neural networks, which extract features from input data by capturing local features based on the convolution layers and integrating global features based on the full connection layers. In the method of Xi, Hopkinson, and Chasmer (2018), they propose a deep 3D fully convolution network to filter both stem and branch points, and Windrim and Bryson (2020) develop a deep learning framework for tree detection, segmentation, and wood reconstruction using the fully convolutional encoder-decoder neural network model. Compared with the traditional machine learning algorithms, deep learning methods need little handcraft features and can adapt to various densities and occlusions in input point clouds, which brings a high accuracy and efficiency in the learning processing. However, learning from point clouds is not an easy task due to the large amount of computation in 3D space, and it is difficult to capture edges, contours and curves information from point clouds by the convolution process as in 2D images.

In order to address issues in the above-mentioned methods, such as the large amount of computation in the 3D convolution process and the limited feature maps in the training process, we contribute a projection layer to convolutional neural works for helping capture geometrical structure information of rotated tree stems, i.e., the linear and cylindrical shape, called R-ProjNet (Rotated-Projection Neural Network). To make the projection effective and correct, we update the projection angle in the learning process by minimizing the loss error of networks. Research related to tree structure analysis, crown segmentation, and 3D modelling can be benefited from the output of our developed network.

2. R-ProjNet formulation and parameters learning

The R-ProjNet uses sampling and convolution layers to capture local features. A key step is to formulate a projection layer to obtain contours and structures of input point clouds. In this work, we formulate the projection layer right before the sampling layer for achieving 2D point clouds to obtain features. The input data are points with coordinate information only, which will be transformed into 2D images at a fixed size. Input scene will be split into regions grouped by the DBSCAN strategy (Xu, Hu, and Xie 2022) using the Euclidean distance information. For each region, they share the same label in the classification, which is regarded as the input of networks. The output shows the label of points from current 3D regions.

Figure 1 shows a shallow R-ProjNet. We denote the projection layer as P_i, the sampling layer as S_i, the convolution layer as C_i, and the full connection layer as F_i, where i represents the ith layer. As shown in input data, the projection of regions from wood points and foliage points are quite different, which provides cues for the separation of wood and foliage points. Wood points are dense and own the same principal direction in a local region, but foliage points are massive and sparse. The optimal 2D points for each
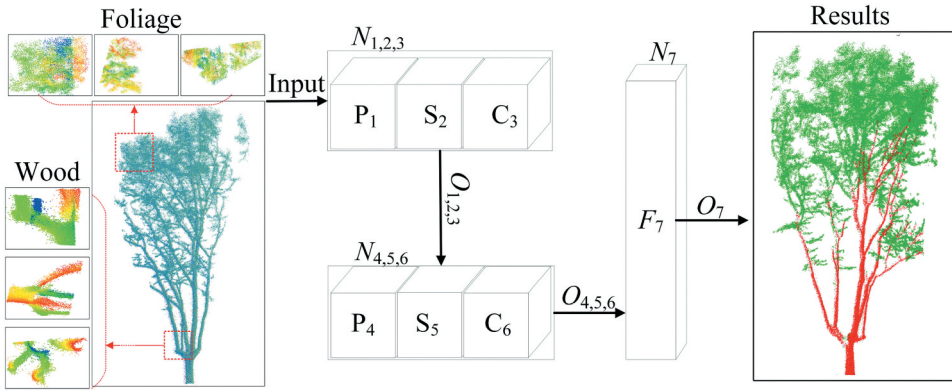
Figure 1. Structure of a shallow R-ProjNet. The color scale in input is based on the elevation of points, which is used to render the height information. Red regions in output stands for wood points and green regions stands for foliage points.

learning process are calculated by our projection layer. For each projection layer, there is one projection matrix to be updated in the learning process.

In order to obtain the optimal 2D point clouds of input data, we add two learnable parameters in the projection layer, i.e., θ and ϕ to show the rotation angle in the vertical and horizontal direction, respectively. The projection matrix is calculated as

$$\mathbf{P} = \begin{pmatrix} \cos\phi_i & ,0, & -\sin\phi_i \cdot \cos\theta_i \\ -\cos\phi_i & ,0, & -\cos\theta_i \cdot \sin\phi_i \\ 0 & ,0, & \cos\phi_i \end{pmatrix} \tag{1}$$

Points are first rotated θ along the vertical direction (z-axis) counterclockwise, and then points are rotated ϕ along the horizontal direction (x-axis). Finally, those rotated points are projected on the xOz plane. As shown in Figure 1, we have two modules P_1-S_2-C_3 and P_4-S_5-C_6. Each module contains one projection layer (P_1 or P_4), sampling layer (S_2 or S_5), and convolution layer (C_3 or C_6). Results are shown in the final output layer after the full connection layer, which can be 1 (target wood points) and 0 (others). Besides the classical parameters of weight and bias in convolution layers, there are two learnable parameters of the developed R-ProjNet to be updated in the learning process, namely the θ and ϕ. We use θ_k^+ to stand for the update result of the rotation angle θ_k in the network. Similarly, for ϕ_k^+ and ϕ_k. Newly added parameters are used to find the optimal projection plane for learning.

In the projection, we want an optimal projection angle which captures more useful information for our classification. The optimal angles can be found by searching a large number of projection angles at the cost of computation. It is worth noting that in the learning stage, we do not require to train samples from every view. This is a significant improvement compared with just using fixed projections in many directions in terms of the algorithm complexity. There is no need to input various parameters for setting projection angles. We train the classifier to obtain the optimal projection angle for each input pattern, which is more flexible and robust to different scenes.

The loss function is based on the cross-entropy and the update of θ and ϕ is based on the backpropagation using the gradient descent strategy as shown in the classical convolutional neural networks. We update the newly added parameters based on the loss error E as shown in Equation (2), where η is a user-defined learning rate based on the classification task.

$$\theta_k^+ = \theta_k - \eta \cdot \frac{\partial E}{\partial \theta_k}, \phi_k^+ = \phi_k - \eta \cdot \frac{\partial E}{\partial \phi_k} \tag{2}$$

In the forward prorogation, we have $O_{i,i+1,i+2} = f(N_{i,i+1,i+2})$ as shown in Figure 1, where the activation function f can be ReLU or LeakyReLU, and we denote $f' = \frac{\partial O_{i,i+1,i+2}}{\partial N_{i,i+1,i+2}}$. Denote E' as the derivative of E with respective to the output of layers, and we present Equation (3) as

$$\frac{\partial E}{\partial \theta_{4,5,6}} = \frac{\partial E}{\partial O_{4,5,6}} \cdot \frac{\partial O_{4,5,6}}{\partial N_{4,5,6}} \cdot \frac{\partial N_{4,5,6}}{\partial \theta_{4,5,6}} \tag{3}$$

Let's continue the propagation process, and we present Equation (4) as

$$\frac{\partial E}{\partial \theta_{1,2,3}} = \frac{\partial E}{\partial N_{1,2,3}} \cdot \frac{\partial N_{1,2,3}}{\partial \theta_{1,2,3}}$$

$$= \frac{\partial E}{\partial O_{4,5,6}} \cdot \frac{\partial O_{4,5,6}}{\partial N_{4,5,6}} \cdot \frac{\partial N_{4,5,6}}{\partial O_{1,2,3}} \cdot \frac{\partial O_{1,2,3}}{\partial N_{1,2,3}} \cdot \frac{\partial N_{1,2,3}}{\partial \theta_{1,2,3}} \tag{4}$$

In the implementation, we update θ based on Equation (2). Similarly, we use the backpropogation rules to obtain $\frac{\partial E}{\partial \phi_{4,5,6}}$ and $\frac{\partial E}{\partial \phi_{1,2,3}}$ to update $\phi_{4,5,6}$ and $\phi_{1,2,3}$, respectively. Subscripts in $\theta_{i,i+1,i+2}$ and $\phi_{i,i+1,i+2}$ represent the layer of the network in the module.

3. Experiments and evaluation

Figure 2 demonstrates the experiment step of our extraction. Each tree is required to be scanned by the LiDAR system to generate the corresponding 3D point clouds. Then,
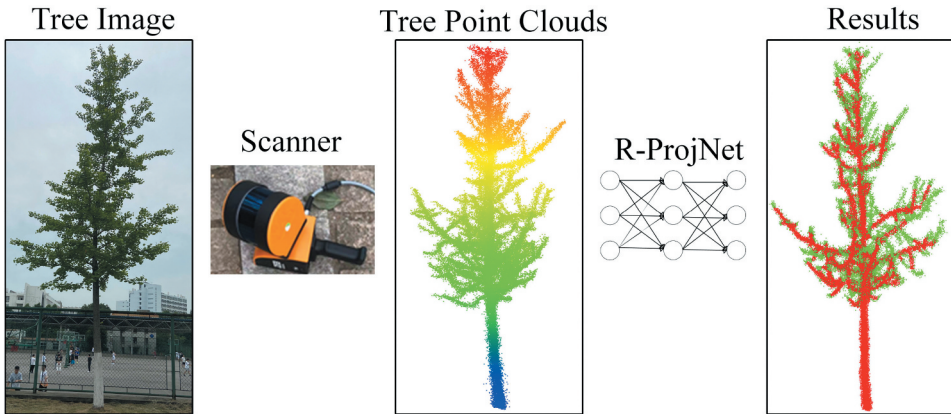

Figure 2. Data collection and processing.

individual tree point clouds are clustered and input for the R-ProjNet for wood point extraction. This section tests the proposed R-ProjNet on handheld and vehicle laser scanning data, respectively, to show our extraction results. In terms of the handheld laser point clouds, data are collected by GeoSLAM ZEB-HORIZON, which scans points at 300,000 points per second at the field of view $360° \times 270°$. The maximum range is 100 m. The range of the scanned noise falls in $\pm$ 30 mm. In the collection, we close the loop as often as possible in order to minimize error and improve the accuracy of the resulting point cloud. This scanner is quite easy to use and suitable for the point collection of street trees. The input scene is located at Linggu Temple, Nanjing, China. Roads are covered by street trees of *Platanus orientalists* as shown in Figure 3(a). Our extraction results are shown in Figure 3(b), which achieves the most wood points from street trees.

In the evaluation, the reference of tree woods is manually segmented from input points through an opensource point visualization software (www.cloudcompare.org). In experiments, we prepare 252 instances of points contain various tree regions as shown in Figure 4, and we set the ratio of the training set, validation set, and test set for each label as 7:1:2, respectively. The training set is used to tune weights for the network, the validation set is prepared for the detection of the overfitting, and the test set is designed for the accuracy calculation.

The evaluation metrics include cross-entropy loss error (Loss) and misclassification error (MCR). We try different network structures for the evaluation, and we show results in Table 1 with the same number of kernels in each layer. The first column 'ID' means the experiment number, 'NoL' means the number of layers in the network, 'PSC' means the number of projection-sampling-convolution modules, 'c' means the kernel size of each convolution layer, 'F' means the number of full connection layer, 'Size' is the size of input data (e.g., 32×32 pixels), 'Loss' is the entropy loss error and 'MCR' is the misclassification error calculated by the ratio of correctly classified objects. As shown in 'Loss' and 'MCR', we have achieved the best performance at ID #2. Experiments from ID #1 to #3 show that R-ProjNet succeeds in achieving high performance in the wood point extraction with fewer layers. Parameters are easy to be learned based on the minimization of Loss error. Experiments from ID #4 to #6 shows that, although we add more full connection layers or enlarge the size of input data, we fail to improve our accuracy greatly. This means that if users add more layers in the learning process, they are required to choose more efficient and effective optimization methods, e.g., dropout and batch normalization strategy. Experiments were done on a Windows 10 Enterprise 64-bit, Intel Core i7-6900k, 3.20
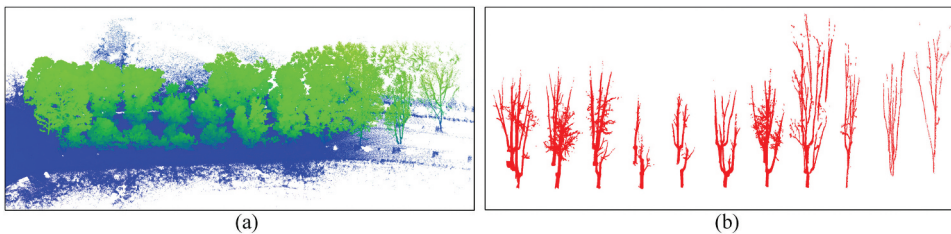

(a)   (b)

Figure 3. Extraction performance of R-ProjNet on handheld laser scanning data. (a) extraction of region of interests from handheld laser scanning data using R-ProjNet. (c) extracted wood points by R-ProjNet.
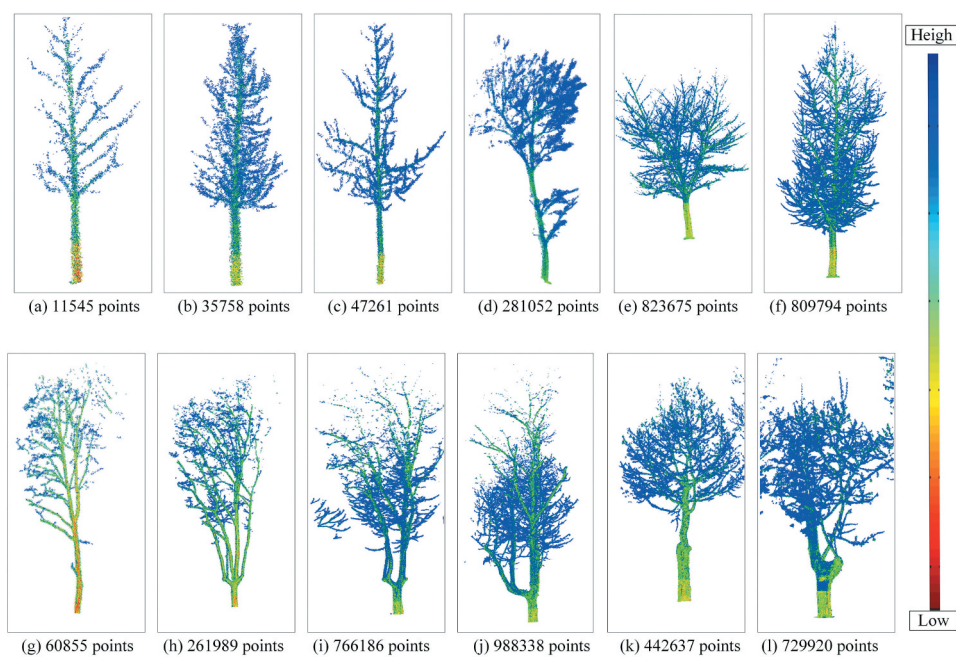
Figure 4. Demonstration of examples used for training. The color scale shows the elevation of points, which is used to render the height information.

Table 1. Accuracy of different network structures.

ID	NoL	PSC	c	F	Size	Loss	MCR
1	7	2	(5,7)	1	32	0.52	0.13
2	10	3	(5,3,3)	1	32	0.41	0.08
3	13	4	(3,3,3,3)	1	32	0.55	0.22
4	11	3	(5,3,3)	2	32	0.57	0.26
5	12	3	(5,3,3)	3	32	0.76	0.35
6	10	3	(5,3,7)	1	64	0.44	0.10

GHz processor with 64 GB of RAM, and computations were carried on Matlab R2019a. We use the matpcl tool (ww2.mathworks.cn/matlabcentral/fileexchange/40382-matlab-to-point-cloud-library) in the coding tasks, which is MATLAB code that allows interfacing with the Point Cloud Library (PCL).

In order to show our improvement on the wood point extraction from Figure 5(a), we choose two methods of wood extraction for the comparison, including Moorthy et al. (2019) and Zhang et al. (2019). It is worth noting that the chosen compared methods are re-implemented by ourselves using Matlab R2019a based on their published algorithm description. In Moorthy et al. (2019), the authors extract Eigen features from points and use the Random Forest algorithm to classify points as shown in Figure 5(b), which fails to classify wood points covered by crowns. In Zhang et al. (2019), the authors use the normal change rate to thin branches, and calculate geometric features for filtering wood points using the height-to-width ratio as shown in Figure 5(c), which works well in wood point segmentation. Our results are shown in Figure 5(d), which achieves the most of wood points from the input handheld laser scanning data with fewer foliage points. The
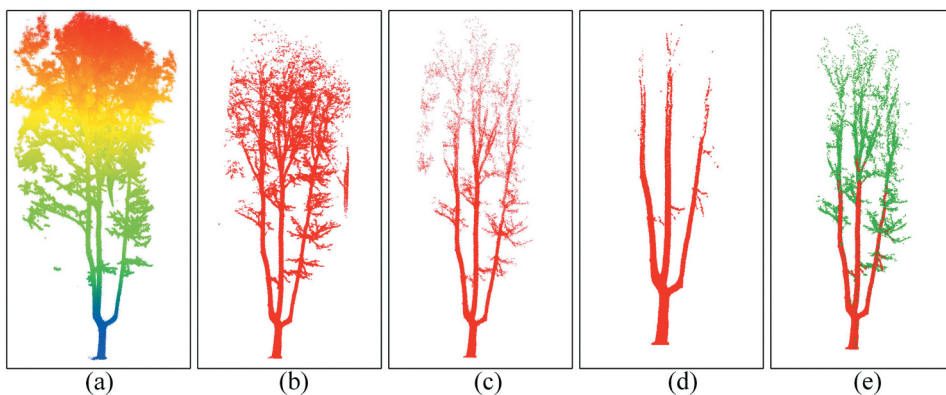
Figure 5. Comparison of the wood point segmentation methods. (a) input data. (b) results of Moorthy et al. (2019). (c) results of Zhang et al. (2019). (d) results of our R-ProjNet. (e) visualization of wood and foliage points based on our results.

visualization of wood and foliage points segmentation based on our results is shown in Figure 5(e).

In order to show our robustness, we test our performance on the wood point extraction of road scenes from the public benchmark (Vallet et al. 2015). The test urban scene is located in Paris collected in January 2013, and the imagery of the test scene is shown in the left of Figure 6. Laser point clouds are acquired by Stereopolis II, a mobile laser scanning system developed at the French National Mapping Agency (IGN). Please refer to http://data.ign.fr/benchmarks/UrbanAnalysis/index.html for more details. The size of the test data is 173 m × 352 m containing around 50 million points as shown in the right of Figure 6.

In order to evaluate the extraction quantitatively, the result of a point is divided into TP (true positive), FN (false negative) and FP (false positive). TP means that a wood point is extracted correctly from the input scene. FN means that a wood point is wrongly detected as the background point. FP means that a background point is wrongly recognized as a wood point. Similarly, the ground truth of wood components for the reference is obtained manually from the input scene attentively through CloudCompare. In the evaluation, we calculate the correctness r, completeness p and F-score as
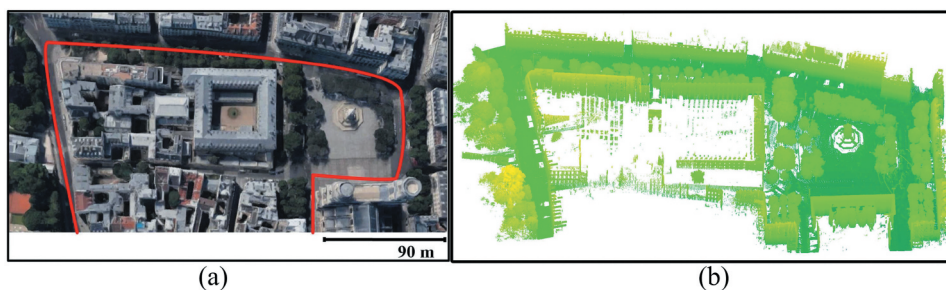

Figure 6. Input data collected by vehicle laser systems. (a) the 2D imagery. (b) 3D point clouds.
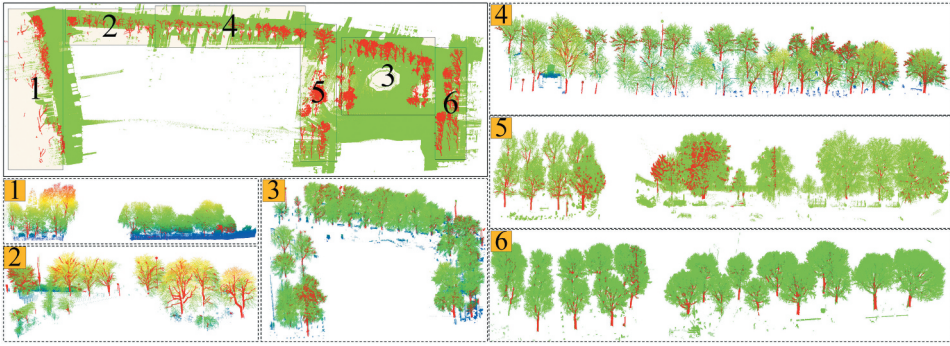
Figure 7. Results of the extraction of wood points from particular regions of the vehicle-based laser scanning data using R-ProjNet.

$$r = \frac{TP}{TP + FP}, p = \frac{TP}{TP + FN}, F - \text{score} = \frac{2 \times TP}{2 \times TP + FP + FN} \quad (5)$$

TP, FP and FN here represent the number of true positives, false positive and false negative, respectively. The correctness measures the ratio of correctly extracted wood components in results, the completeness measures the percentage of correctly extracted wood components in the reference. F-score is the harmonic mean of correctness and completeness. The input single tree data are obtained by optimizing supervoxels for grouping points from the same individual trees (Xu et al. 2018). There are 182 trees in the test scene and we extract 167 fully individual instances from the input data as shown in Figure 7. We demonstrate results in six regions to highlight our performance. The average point-based correctness, completeness and F-score are 90.4%, 91.5% and 0.91, respectively, which is better than the published wood points detection accuracy from Xia et al. (2015) (F-score 0.90), Fan, Chenglu, and Jonathan (2016) (F-score 0.88) and Guan et al. (2016) (F-score 0.89). In this case, we also test the results of training process by setting fixed projection angles for every 30 degrees. The training stage incurs lots of feature maps, and we ignore parameters θ and ϕ. Results show that the learning correctness, completeness and F-score are decreased to 79.1%, 76.7% and 0.78, respectively. Although we can improve the classification accuracy by using a small-angle interval, it is a tough work for searching the best angles efficiently. Our misclassification caused by street lamps and traffic signs, which required a post-process step to remove false woods. Although methods based on quantitative structure models, e.g., TreeQSM (Raumonen et al. 2013), provide 3D branch models conveniently, these methods work slowly for dense point clouds. Besides, they highly rely on the structure of branches and tend to fail when tree branches are incomplete or occluded. They usually connect spatially neighbouring tree branches directly using curved pipes.

4. Conclusions

In this work, we develop a new projection convolutional neural network for the wood point extraction called R-ProjNet. The projection is based on the rotation of point clouds along different axis and planes. In order to obtain the optimal projection for the

subsequent sampling and convolution process, we formulate two parameters in the proposed R-ProjNet for tuning the projection. Those two parameters can be updated in the learning process by minimizing errors. This work indicates that first, mobile laser scanning systems can capture 3D information of trees correctly, which provides an effective way to analyse 3D space. Second, the added projection layer can help convolutional neural networks capture structure information, such as linear and cylindrical shapes, for detecting wood points. Finally, the formulated parameters in the projection layer provide more efficient 2D points for the training task at a few layers. Experimental results show that we have achieved loss and misclassification errors of 0.41 and 0.08, respectively, on the collected handheld laser scanning point clouds, and we obtained the correctness, completeness and F-score of 90.4%, 91.5% and 0.91, respectively, on the vehicle laser scanning data.

Although we have achieved high performance in experimental scenes, the proposed network has one limitation to be tackled in future work. For complex learning tasks, i.e., more labels to be classified, one is required to add more layers to capture features, but the proposed network is difficult to be backpropagated when there are more layers. Because we introduce more parameters in the training.

Disclosure statement

Funding

ORCID

Sheng Xu http://orcid.org/0000-0002-9017-1510

References

Balenović, I., X. Liang, L. Jurjević, J. Hyyppä, A. Seletković, and A. Kukko. 2021. "Hand-Held Personal Laser Scanning–Current Status and Perspectives for Forest Inventory Application." *Croatian Journal of Forest Engineering: Journal for Theory and Application of Forestry Engineering* 42 (1): 165–183. doi:10.5552/crojfe.2021.858.

Chen, Y., S. Wang, J. Li, L. Ma, R. Wu, Z. Luo, and C. Wang. 2019. "Rapid Urban Roadside Tree Inventory Using a Mobile Laser Scanning System." *IEEE Journal of Selected Topics in Applied Earth Observations and Remote Sensing* 12 (9): 3690–3700. doi:10.1109/JSTARS.2019.2929546.

Fan, W., W. Chenglu, and L. Jonathan. 2016. "Automated Extraction of Urban Trees from Mobile Lidar Point Clouds." 2nd ISPRS International Conference on Computer Vision in Remote Sensing (CVRS 2015), International Society for Optics and Photonics, Xiamen, China, vol 9901, p. 99010. https://doi.org/10.1117/12.2234795.

Guan, H., Y. Yu, J. Li, and P. Liu. 2016. "Pole-Like Road Object Detection in Mobile Lidar Data via Supervoxel and Bag-Of-Contextual-Visual-Words Representation." *IEEE Geosci Remote S* 13 (4): 520–524.

Hui, Z., S. Jin, Y. Xia, L. Wang, Y. Y. Ziggah, and P. Cheng. 2021. "Wood and Leaf Separation from Terrestrial Lidar Point Clouds Based on Mode Points Evolution." *Isprs Journal of Photogrammetry and Remote Sensing* 178: 219–239. doi:10.1016/j.isprsjprs.2021.06.012.

Hu, C., Z. Pan, and T. Zhong. 2020. "Leaf and Wood Separation of Poplar Seedlings Combining Locally Convex Connected Patches and K-Means++ Clustering from Terrestrial Laser Scanning Data." *Journal of Applied Remote Sensing* 14 (1): 1. doi:10.1117/1.JRS.14.018502.

Li, Q., P. Yuan, X. Liu, and H. Zhou. 2020. "Street Tree Segmentation from Mobile Laser Scanning Data." *International Journal of Remote Sensing* 41 (18): 7145–7162. doi:10.1080/01431161.2020.1754495.

Moorthy, S. M. K., Y. Bao, K. Calders, S. A. Schnitzer, and H. Verbeeck. 2019. "Semi-Automatic Extraction of Liana Stems from Terrestrial Lidar Point Clouds of Tropical Rainforests." *Isprs Journal of Photogrammetry and Remote Sensing* 154: 114–126. doi:10.1016/j.isprsjprs.2019.05.011.

Moorthy, S. M. K., K. Calders, M. B. Vicari, and H. Verbeeck. 2020. "Improved Supervised Learning-Based Approach for Leaf and Wood Classification from LiDar Point Clouds of Forests." *IEEE Transactions on Geoscience and Remote Sensing* 58 (5): 3057–3070. doi:10.1109/tgrs.2019.2947198.

Raumonen, P., M. Kaasalainen, M. Åkerblom, S. Kaasalainen, H. Kaartinen, M. Vastaranta, M. Holopainen, M. Disney, and P. Lewis. 2013. "Fast Automatic Precision Tree Models from Terrestrial Laser Scanner Data." *Remote Sensing* 5 (2): 491–520. doi:10.3390/rs5020491.

Sun, C., C. Huang, H. Zhang, B. Chen, F. An, L. Wang, and T. Yun. 2022. "Individual Tree Crown Segmentation and Crown Width Extraction from a Heightmap Derived from Aerial Laser Scanning Data Using a Deep Learning Framework." *Frontiers in plant science* 13. doi:10.3389/fpls.2022.914974.

Vallet, B., M. Brédif, A. Serna, B. Marcotegui, and N. Paparoditis. 2015. "Terramobilita/Iqmulus Urban Point Cloud Analysis Benchmark." *Computers & Graphics* 49: 126–133. doi:10.1016/j.cag.2015.03.004.

Vatandaşlar, C., and M. Zeybek. 2021. "Extraction of Forest Inventory Parameters Using Handheld Mobile Laser Scanning: A Case Study from Trabzon, Turkey." *Measurement* 177 (109): 328. doi:10.1016/j.measurement.2021.109328.

Wang, D. 2020. "Unsupervised Semantic and Instance Segmentation of Forest Point Clouds." *Isprs Journal of Photogrammetry and Remote Sensing* 165: 86–97. doi:10.1016/j.isprsjprs.2020.04.020.

Windrim, L., and M. Bryson. 2020. "Detection, Segmentation, and Model Fitting of Individual Tree Stems from Airborne Laser Scanning of Forests Using Deep Learning." *Remote Sensing* 12 (9): 1469. doi:10.3390/rs12091469.

Xia, S., C. Wang, F. Pan, X. Xi, H. Zeng, and H. Liu. 2015. "Detecting Stems in Dense and Homogeneous Forest Using Single-Scan Tls." *Forests* 6 (11): 3923–3945. doi:10.3390/f6113923.

Xi, Z., C. Hopkinson, and L. Chasmer. 2018. "Filtering Stems and Branches from Terrestrial Laser Scanning Point Clouds Using Deep 3-D Fully Convolutional Networks." *Remote Sensing* 10 (8): 1215. doi:10.3390/rs10081215.

Xu, Y., C. Hu, and Y. Xie. 2022. "An Improved Space Colonization Algorithm with Dbscan Clustering for a Single Tree Skeleton Extraction." *International Journal of Remote Sensing* 43 (10): 3692–3713. doi:10.1080/01431161.2022.2102950.

Xu, S., N. Ye, S. Xu, and F. Zhu. 2018. "A Supervoxel Approach to the Segmentation of Individual Trees from Lidar Point Clouds." *Remote Sensing Letters* 9 (6): 515–523. doi:10.1080/2150704X.2018.1444286.

Yun, T., K. Jiang, G. Li, M. P. Eichhorn, J. Fan, F. Liu, B. Chen, F. An, and L. Cao. 2021. "Individual Tree Crown Segmentation from Airborne Lidar Data Using a Novel Gaussian Filter and Energy Function Minimization-Based Approach." *Remote Sensing of Environment* 256 (112): 307. doi:10.1016/j.rse.2021.112307.

Zhang, W., P. Wan, T. Wang, S. Cai, Y. Chen, X. Jin, and G. Yan. 2019. "A Novel Approach for the Detection of Standing Tree Stems from Plot-Level Terrestrial Laser Scanning Data." *Remote Sensing* 11 (2): 211. doi:10.3390/rs11020211.